Non-linear Dynamics of Multilayered Sandwich Beams

J. Awrejcewicz[1], V. A. Krys'ko[2] and V. Bochkarev[2]

[1] *Technical University of Lodz, Department of Automatics and Biomechanics, 1/15 Stefanowskiego St., 90-924 Lodz, Poland, tel/fax: +(4842) 6312225, awrejcew@ck-sg.p.lodz.pl.*
[2] *Saratov State University, Department of Mathematics, 41005 Saratov, Russia.*

Abstract

In this paper dynamics of physically dissipative non-linear multi-layer sandwich of three beams is analysed. The boundary conditions are arbitrary. The transversal load can be applied either simultaneously to all beams or separately to each of the beams. The finite difference method is used to solve the governing equations. Different types of beam material are considered: ideally elastic-plastic, elastic-plastic with linear strenghtness, and pure aluminum.

1 Introduction

Damping and dissipating energy of a beam (or of sandwich beams) have been studied by a large number of researchers. Mead and Markus [1-3] studied a sixth order differential equation of motion in terms of the transverse displacement of a beam with arbitrary boundary conditions, and it serves as a classical method of modeling and describing damped three-layer beams and plates (see also [4, 5]). In the [6, 7] the experimental results from a cantilever beam under impact loading and with an operating four-bar mechanism are reported. Both experimental and analytical results for the compressional vibration of an elastic-viscoelastic-elastic three-layer sandwich beam are reported by Sisemore and Darveness [8].

Another research direction includes the free vibration of beams with concentrated masses (see Chen [9] and Goel [10]). The natural frequencies of a cantilevered beam with a slender tip mass are investigated in [11, 12]. The Euler-Bernoulli and Timoshenko beam models are used in [13] to analyse the free vibration of simply supported and cantilever beams with distributed mass. Two distributed masses in-span attached to a beam are studied in [14]. A mass carried by two different beam segments is studied by Kopmaz and Telli [15].

Free vibration analysis of non-uniform beams with an arbitrary number of cracks and concentrated masses is carried in the Li paper [16]. The eigenvalue equation of a non-uniform beam with any two kinds of end support, any finite number of cracks and with concentrated masses are determined from a second order determinant, which significantly saves the computational effort.

A non-linear model analysis approach, based on invariant manifold theory, is proposed by Shaw and Pierre [17], and then used by Yie et al. [18].

Three identification methods of non-linear model behaviour of an externally excited cantilever beam are proposed and discussed in [19]. The propagation of structural waves, on an infinitely long periodically supported Timoshenko beam, are studied in [20]. The power series expansion of displacement components method, yielding a set of fundamental dynamic equations of a one-dimensional higher order theory for a laminated composite beams subjected to axial stress derived through Hamilton's principle, is applied by Matsunaga [21]. The approach introduced is used for the analysis of natural frequencies and buckling stresses of laminated composite beams, taking into account the complete effects of transverse shear, normal stresses and rotatory interia.

The dynamic stability of a stepped beam subject to a moving mass is analysed in the [22]. It is shown that the stability of certain beam models can be improved by providing the beam with appropriately spaced steps.

Two simple systems comprising straight uniform Euler-Bernoulli beams in which there are internal self-balancing axial loads are analysed by Mead [23].

Investigation of chaos exhibited by beams with different boundary conditions is reported in series of [24-29]. Different aspect of non–linear longitudinal or transverse vibrations of beams subject to periodical longitudinal or transverse excitations are analyzed.

In this work a system consisting of three sandwich beams in a dissipative medium is analysed. The beam material is assumed to be non-linear and elastic.

2 Problem formulation and computational algorithm

Dynamic interaction of three sandwich beams with clearance in their equilibrium state is analyzed. The kinematic J. Bernoulli hypothesis is assumed for the formulation of the governing equations. It is assumed that in a contact zone the beams slip freely. A contact pressure (load) is found using Winkler's hypothesis [30]. Finally, one of the beams is subjected to periodic transverse load excitation.

The beam occupies the following domain in a three dimensional space:

$$G = \left\{ (x, y, z) \;\middle|\; 0 \le x \le a,\;\; 0 \le y \le b,\;\; -\frac{h}{2} \le z \le \frac{h}{2} \right\},$$

and the following notation is used: h - beam thickness; h_{10} - beam thickness in a center; w_l - beam deflection; E_l - elasticity modulus; b_l - beam width; t - time; ε_l - damping coefficient; u - beam length; ρ_l - maternal density; p_l - clearance between beams (l = 1, 2, 3); σ_l - Poisson's coefficient; e_i - deformation intensity; σ_i - stress intensity; e_{sl} - intensity of flow deformation; σ_s - intensity of stress flow deformation; K - volume elasticity modulus.

The following non–dimensional parameters are introduced:

$$x = \bar{x}a, \quad y = \bar{y}b, \quad z = \bar{z}\,h_{0l}, \quad h_l = \bar{h}_l\,h_{0l}, \quad w_l = \bar{w}_l\,h_{0l}, \quad E_l = \bar{E}_l\,G_{0l}, \quad b_l = \bar{b}_l\,b_{0l},$$

$$p_l = \bar{p}_l\,h_{0l}.$$

The x coordinate is measured beginning from the left plate end and is extended along the beam axis, whereas z axis is measured beginning from the mean curve down.

The beams motion is governed by the following non–dimensional equations

$$h_l = \frac{\partial^2 w_l}{\partial t^2} + \varepsilon_l \frac{\partial w_l}{\partial t} = -L_l(w_l) - q_{kl} - q_l, \quad l = 1, 2, 3. \tag{1}$$

Now and later the index $l = 1$ corresponds to the top beam, $l = 2$ corresponds to the middle beam, and $l = 3$ refers to the bottom beam.

The operators $L_l(w_l)$ are defined via the formula

$$L_l(w_{l_i}) = \frac{\partial^2}{\partial x^2}\left[(b_1 P_l(x)) \frac{\partial^2 w_l}{\partial x^2} \right], \tag{2}$$

where:

$$P_l(x) = \int_{\frac{-h}{2}}^{\frac{h}{2}} E_l z^2\, dz\,. \tag{3}$$

The method of variation of the elasticity parameters is further applied in order to include physical material nonlinearities. In accordance with this method the elasticity modulus is coupled with the Poisson's and deformation moduli via the relation

$$E = \frac{9KG}{3K + G}\,. \tag{4}$$

The modulus K is assummed to be constant and equal to $1.94G_{0l}$. Recall that in strain theory the shear modulus is defined via the formula

$$G = \frac{1}{3}\frac{\sigma_i(e_i)}{e_i}. \tag{5}$$

An arbitrary strain diagram of the beam material $\sigma_i(e_i)$ can be used. For example, it can be represented by one of the following choices [31]:

1. Ideally elastic–plastic material

$$\sigma_i = 3G_{0l}e_{sl}, \quad \text{for} \quad e_i < e_{sl},$$
$$\sigma_i = \sigma_s, \quad \text{for} \quad e_i \geq e_{sl}. \tag{6}$$

2. Elastic – plastic material with linear strengthness

$$\sigma_i = 3G_{0l}e_{sl}, \quad \text{for} \quad e_i < e_{sl},$$
$$\sigma_i = 3G_{0l}e_{sl} + 3G_l(e_i - e_{sl}), \quad \text{for} \quad e_i \geq e_{sl}. \tag{7}$$

3. Diagram for pure aluminum has the form

$$\sigma_i = \sigma_s\left[1 - \exp\left(-\frac{e_i}{e_{sl}}\right)\right] \tag{8}$$

The deformation intensity is governed by the following relation

$$e_i = \frac{\sqrt{2}}{3}\left[(e_{xx} - e_{yy})^2 + (e_{yy} - e_{zz})^2 + (e_{xx} - e_{zz})^2 + \frac{3}{2}e^2{}_{xy}\right]^{\frac{1}{2}}$$

Neglecting (for a beam) the components e_{yy} and e_{zz} one obtains

$$e_i = -\frac{2}{3}e_{xx}, \quad \text{or} \quad e_i = -\frac{2}{3}z\frac{\partial^2 w}{\partial x^2}. \tag{9}$$

The boundary conditions of the beams system are arbitrary. In particular, one may apply free, simple support or clamping conditions. The initial conditions have the form:

$$\frac{\partial w_l(x,0)}{\partial t} = F_l(x), \qquad w_l(x,0) = f_l(x), \qquad l = 1, 2, 3 \tag{10}$$

where: F_l and f_l are function of velocities and deflection distributions at the initial time instant, respectively. The transversal load can be applied either to all beams simultaneously or it can act on each of the beams separately. The load distributions along the beam and in time can be taken arbitrarily. In addition, a jump phenomenon (the beams separation phenomena) during beams interactions is included. The contact stresses are defined by the relations

$$q_{kl} = (-1)^l k_1 \frac{E_1}{h_1}\left(w_1 - p_1 - w_2\frac{h_{02}}{h_{01}}\right)\psi_1, \qquad l = 1, 2, \tag{11}$$

$$q_{kl} = (-1)^{i+1} k_2 \frac{E_2}{h_2}\left(w_2 - p_2 - w_3\frac{h_{03}}{h_{02}}\right)\psi_2, \qquad l = 2, 3, \tag{12}$$

where: k_1 is the proportionality coefficient between contact pressure and clamping; the function ψ_1 defines a contact zone dimension and is found from the formula

$$\psi_l = \frac{1}{2}\left[1 + sign\left(w_l - p - w_{l+1}\frac{h_{0l+1}}{h_{0l}}\right)\right]. \tag{13}$$

In order to integrate equations (1) the finite difference method of approximation $O(h^2)$ is applied. The space $D=\{(x,t)\mid 0\le x\le 1,\ 0\le t\le T\}$ is covered by the rectangular mesh $x_i=ih_x, t_j=jh_t$ $(i=0,1,2..n;\ j=0,1,2,..)$, where $\Delta x_i=x_{i+1}-x_i=h_x=1/n_x$ (n_x is an integer) and $h_t=t_{j+1}-t_j$. Between the nodes the differential equation (1) is approximated by finite–difference relations. In order to increase the accuracy results of the symmetric formulas for derivative are applied. After a series of easy transformation for a beam with beam number l one obtains

$$w_{li,j+1}=\frac{1}{1+\dfrac{\varepsilon_l h_t}{2h_{li}}}\left[2w_{li,j}+\left(\frac{\varepsilon_l h_t}{2h_{li}}-1\right)w_{li,j}+\frac{h_t^2}{h_{li}}\left((-1)^l q_{kl}+L(w_l)_{i,j}\right)\right],$$

where:

$$L(w_l)_{i,j}=[p_{li+1}w_{li+2,j}-2(p_{li+1}+p_{li})w_{li,j}+(p_{li+1}+4p_{li}-p_{li-1})w_{li,j}-2(p_{li}+p_{li-1})w_{li-1,j}+$$
$$p_{li-1}w_{li-2,j}]/h_x^4+k_{fl}w_{li,j}$$

$$p(x)=b_l P(x),\quad (l=1,2)$$

Note that a three layer system is obtained. In order to compute $w_l(x,t)$ on the layer $(j+1)$ the values $w_l(x,t)$ in two other layers, $j-th$ and $(j-1)$-th, are used. First the $w_l(x,t)$ values of a fictive layer with number $j=-1$ are taken in order to initiate computations. Note also that a derivative in the initial conditions (10) is substituted by a finite difference relation.

An application of the variation of parameters method requires a splitting of the beam along its thickness into n_z layers.

Next, for the node x_j of each layer, the deformation intensity is found using the formula (9) on each time step of the computation. The elasticity modulus is defined via formulas (4), (5) and one of the expressions (6)-(8), and next the integral (3) is computed using the Simpson's method.

3 Numerical results

As an example the case when the top and lower beams are simply supported through balls on both ends is considered:

$$\frac{\partial w_1(0,t)}{\partial x}=w_1(0,t)=\frac{\partial w_1(1,t)}{\partial x}=w_1(1,t)=0,\quad l=1,3. \tag{14}$$

The middle beam is treated as the cantilever one:

$$\frac{\partial w_2(0,t)}{\partial x}=w(1,t)=0;\frac{\partial^2 w_2(1,t)}{\partial x^2}=\frac{\partial}{\partial x}\left(b_2P(x)\frac{\partial^2 w_2(1,t)}{\partial x^2}\right)=0 \tag{15}$$

The following initial conditions are applied

$$F_l(x)=f_l(x)=0,\quad i=1,2,3\quad (0\le x\le 1), \tag{16}$$

and the transverse load drives only the top beam in a harmonic way:

$$q_1=q_{10}\cos(\omega t). \tag{17}$$

The algorithm used to solve the equation governing beam vibrations is investigated from the point of view of both space and time meshes. The relaxation method is used to find the deflection in the center of a simply supported beam after the sudden application of uniformly distributed load along its length $(q_{10}=0.15)$.

The computational results, depending on both the mesh step in time h_t (along horizontal direction), and the number of beams splitting along its length n_x (along vertical direction), are reported in Table 1.

Table 1. Deflection of the beam center for different mesh steps in time h_t and along its length n_x.

	$h_t = 0{,}001$	0,0001	0,00004	0,00002
$n_x = 10$	0,02362	0,02362	0,02362	0,02362
16	0,02351	0,02351	0,02351	0,02351
20	0,02348	0,02348	0,02348	0,02348
24	0,02347	0,02347	0,02347	0,02347
28	0,02346	0,02346	0,02346	0,02346

Note that the center deflection, found analytically for a static approach (9), is equal to 0.2343. Analysis of these results implies that a deflection does not depend on the computational time step, at least for the intervals investigated. However, it depends essentially on the number of splittings along the spatial coordinate. On the other hand, a solution to the problem leads to conclusion that, for $h_t \le 0.0001$ and for a given n_x, one obtains the same behavior for the interaction of the beams. However, the results depend strongly on n_x, which may have the following physical interpretation. Observe that an application of a beam reduces the problem to the analysis of a multibody system dynamics with finite degrees of freedom instead of a continuous system governed by partial differential equations.

Hence, vibration of a number of nodes along the thickness direction yields in practice to the solution of another problem.

The results obtained suggest the following choice of computational steps. The spatial step along the x coordinate is set equal to $0.05\,(n_x = 20)$, and the time step is taken as $2 \cdot 10^{-5}$. The number of layers along z coordinate is taken equal to $n_z = 20$. The computations are carried out for $k_1 = k_2 = 2000,\ a \le t \le 120;$ the clearances between beams are assumed to be $p_1 = p_2 = 0.05$. The material of the beams is assumed to be elastic-plastic with linear strain hardening (7). Flow deformation intensity is assummed to be $e_{s1} = e_{s2} = e_{s3} = 0.1$ for all three beams, and the excitation frequency $\omega = 0.80$.

Note, that a non-linear elastic problem is solved instead of the elastic-plastic one, when the load-relief curve is without hysteresis. Of course, this is a simplification of the real deformation process of the beams.

4 All of three beams are linearly elastic $(\mathbf{G_1 = G_2 = G_3 = 1})$

The time movement of the surfaces of contact pressure are only reported. The damping coefficients $\varepsilon_1 = \varepsilon_2 = \varepsilon_3 = 1.4$. Note that all characteristics are taken for center points in the cases of freely supported beams (on balls), and for the end point of the cantilever beam.

For small load values $q_{10} < 0.34$ only the top beam vibrates, and the frequency spectrum includes only the external excitation frequency ω. With the load increase, after an impact between top and middle beams, the latter starts to vibrate. The top beam exhibits quasi-periodic vibrations. Although in the frequency spectrum the frequency 2ω is observed, but its amplitude is much more smaller than that corresponding to the fundamental frequency. A deflection surface of the top beam creates a regular wave form structure. The middle beam vibrates in a quasi-periodical manner, and in the spectrum the fundamental frequency ω and integral multiple frequencies $2\omega, 3\omega$ appear. Its deflection surface is much more complicated than that of the top beam. The contact zone between them occurs in their central parts.

The described qualitative behavior takes place until $q_{10} = 0.596,$ when the middle beam touches the lower one. This event causes a qualitative change in the type of vibration of all three beams: the first period doubling appears. In the power spectrum the frequency components $\omega/2,\ 3\omega/2,$ and so on, are visible. Note that in the top beam the fundamental frequency ω dominates in its power spectrum. In the middle beam the amplitudes corresponding to the frequencies mentioned above are similar. Therefore, the

phase portrait changes slightly for the first beam, whereas loops appear in the phase portrait of the second beam. Two sets of points are observed in the Poincaré sections. The sudden triple bifurcation, just after vibration occurrence, is observed in the third beam.

The deflection surface of the top beam remains practically unchanged, but this can not be said of the second beam. Characteristic properties of a contact zone between the two top beams are conserved, only its width is increased. An interaction between middle and top beams appears at the end of the consol beam. The phase portrait and power spectrum prove that a slight degree of chaos appears. Increasing the load up to $q_{10} = 0.606$ the frequency components corresponding to a triple bifurcation appear also in both top and middle beams. The physical explanation follows: the amplitude of the lower vibrations increases, and hence it more strongly interacts with two remaining beams. Simultaneously, in the power spectra of all three beams the components corresponding to the first Hopf bifurcation appear. The deflection surfaces of the beams are practically conserved. The contact zone between top and middle beams change, and contact takes place on some intervals along the beams length (Fig. 1).

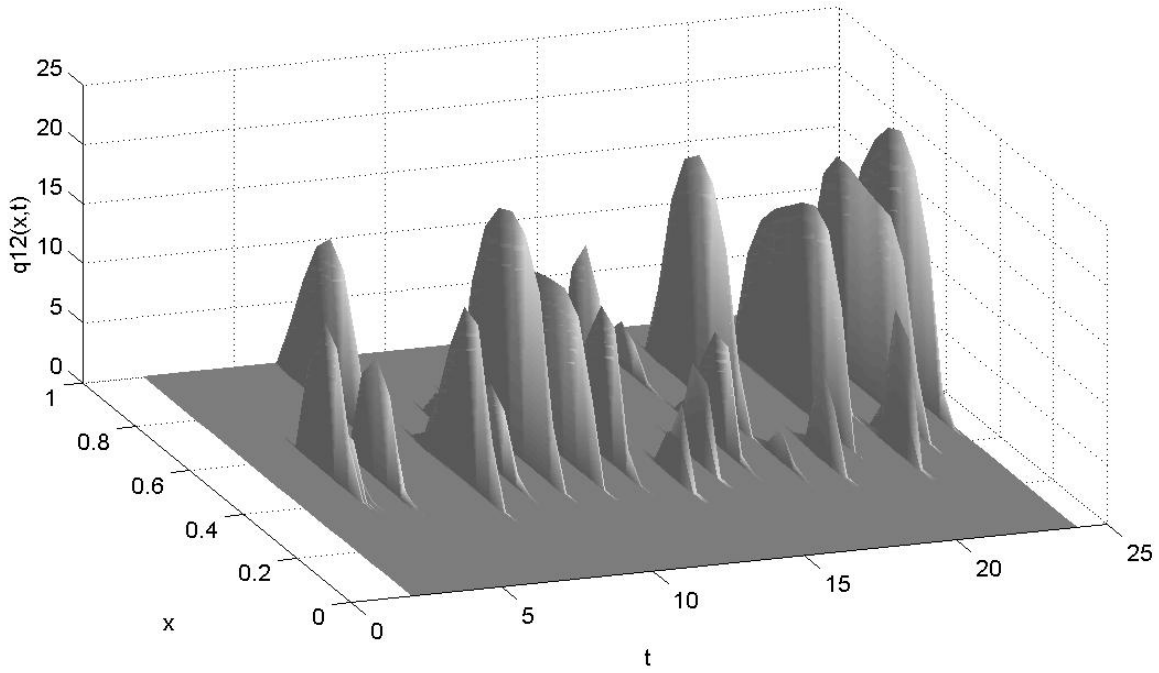

Figure 1. Contact pressure between the second and the third beams $q_1 = 0.65 \quad t = 2 - 24$.

A collapse of the triple bifurcation with a simultaneous occurrence of period doubling (Hopf) bifurcation occurs for $q_{10} = 0.612$. However, the frequency components produced by this bifurcation are essentially smaller in comparison to the analogous components of the first bifurcation. Therefore, the fundamental associated characteristics, like amplitude characteristics, Poincaré section, phase portrait and power spectra, remain practically unchanged. Furthermore, for $q_{10} \geq 0{,}614$, in the spectra of second and lower beams, noisy components appear. All beams are in the synchronization regime within the frequencies of the secondary Hopf bifurcation. The points of the Poincaré sections display irregularity. The vibration picture is conserved up to $q_{10} = 0.65$ with a simulteneous increase of noisy components. The deflection character and interaction zones of the beams do not change (see Fig. 2).

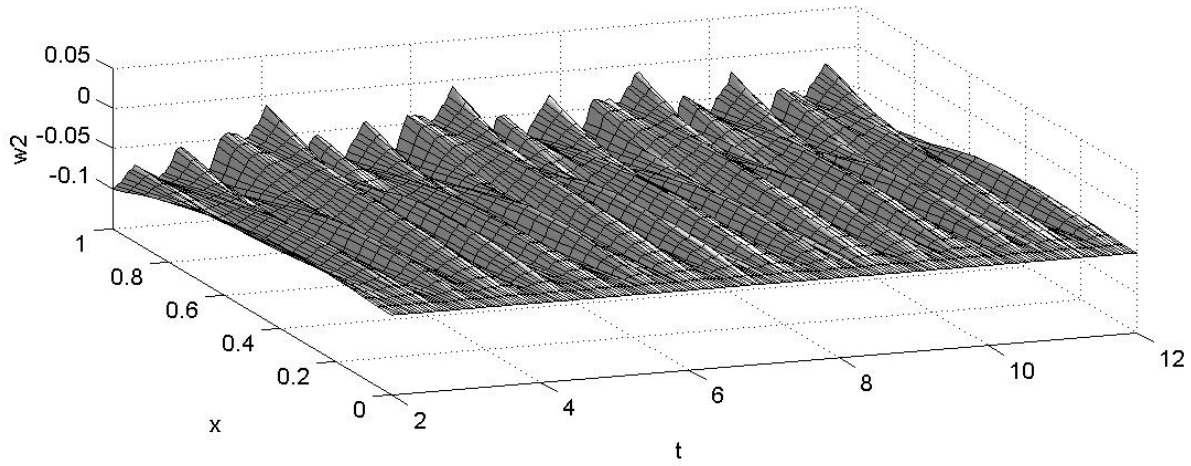

Figure 2. Surface on deflections $q_1 = 0.62$ $t = 2-12$.

Next, second Hopf bifurcation is collapsed, and vibration of all beams is synchronized on the fundamental frequency ω, and all other frequency components are integral multiples, i.e. $2\omega, 3\omega,$ and so on. Furthermore, when the load increases up to $q_{10} = 2$, the motion of the second beam becomes chaotic, what is displayed by the "wash out" phase portraits and Poincaré sections. On the other hand, those characteristics exhibit the regularization of vibrations of top and lower beams. The beams interaction changes qualitatively. The contact zones between all three beams are split into intervals (Fig. 3).

To conclude, the following scenarios leading to chaos are reported: one frequency vibration (harmonic regime), first Hopf bifurcation, triple bifurcation and its collapse, second Hopf bifurcation and its collapse, transition to chaos. This scenario is not similar to that of the Feigeubaum transition: the bifurcation sequence is finite, and in addition in spite of a period doubling bifurcation, a triple bifurcation is observed.

5 All three beams are non-linearly elastic $(\mathbf{G_1 = G_2 = G_3 = 0})$

The vibration characteristics are located in the way similar to the linearly elastic case. In addition, the dependence on time of the deformation intensity is reported in $e_i(t)$. This is defined on the beams surfaces in the case of free (balls) support, and clamping-for the cantilever beam.

The solid curve corresponds to the flow deformation intensity e_{sl}. Similar to the previous case, the top beam exhibits quasi-periodic vibrations. This can be easily observed in the phase portrait and the power spectrum. Note that deformation intensity exceeds $e_{s1,}$ i. e. the deformation intensity achieves a horizontal part of the deformation diagram (7). Increasing q_{10} excites the second beam. The top beam exhibits quasi-harmonic vibrations, whereas the second beam vibrates quasi-periodically. In the power spectrum of the latter, the components ω and 2ω are observed. Since the second component is essentially larger then the first one, the amplitude characteristics are qualitatively different in comparison with the case of harmonic vibrations. For $q_{10} = 0.75$ the first period doubling occurs and the components $\omega/2$, $3\omega/2$, and so on, appear.

(a)

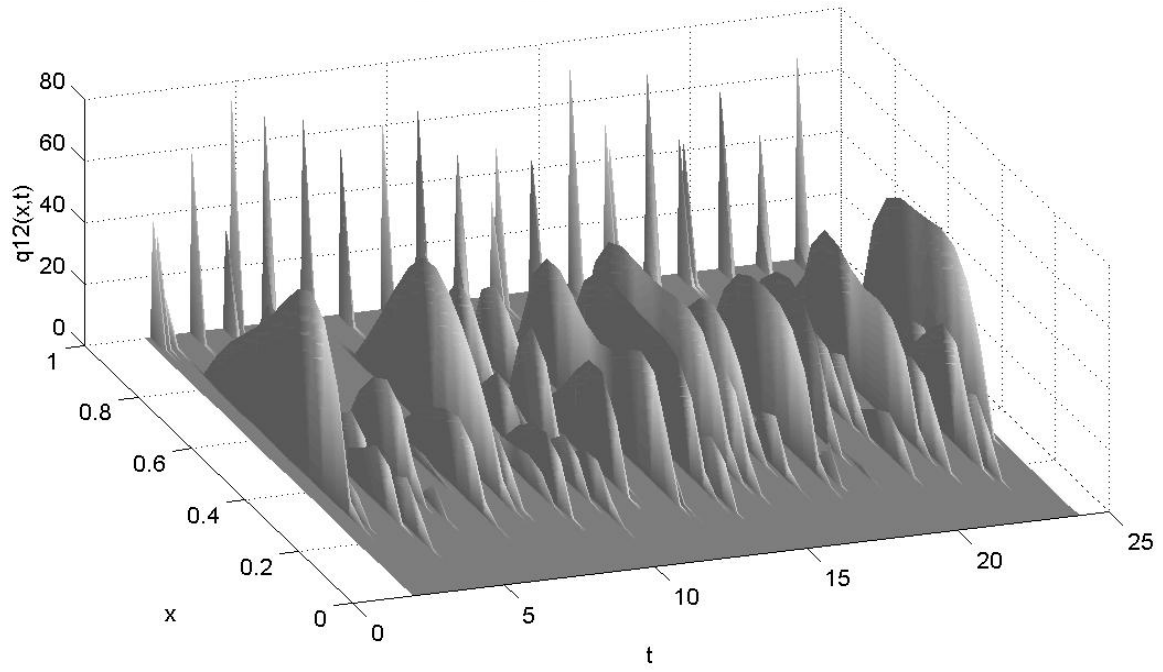

(b)

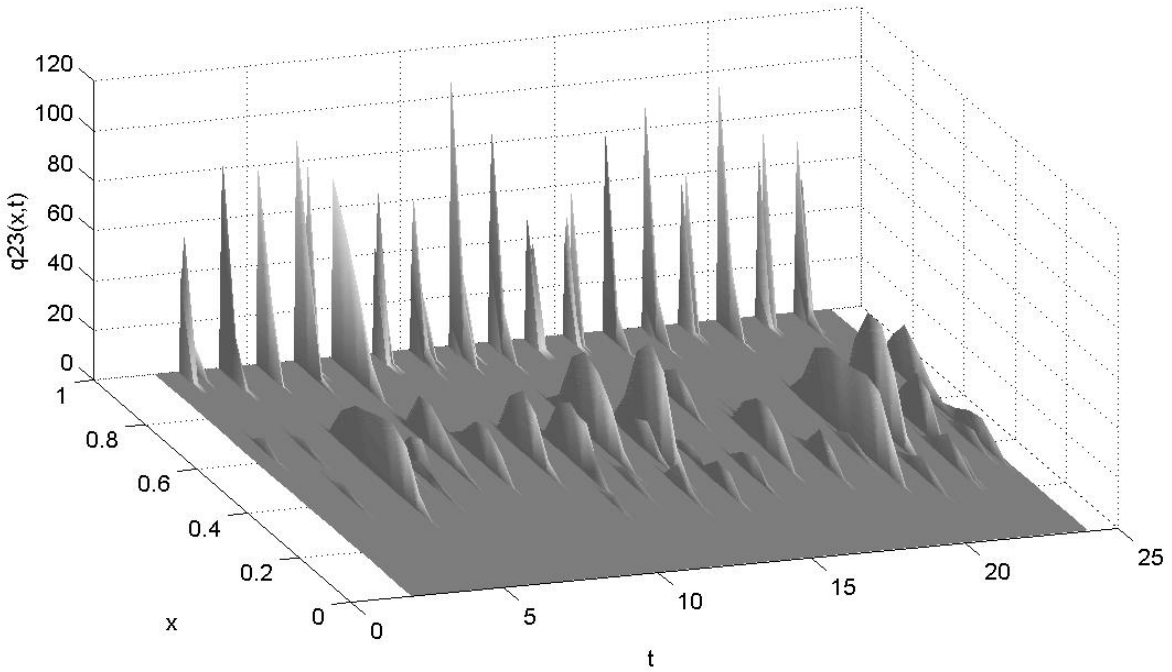

Figure 3. Contact pressures between the first and the second (a) and the second and the third (b) beams $q_1 = 2 \quad t = 2 - 24$.

However, the quasi components are very small for the first beam, so its vibrations remain quasi-harmonic. For the second beam, those components are large and the vibrations more complex, are shown by the amplitude characteristics and the phase portraits. In the Poincaré section, with respect to the period of exciting force, two sets of points occur, instead of one point observed for a smaller load. Both beams

achieve the horizontal part of the deformation diagram, which is exhibited by the characteristics $e_i(t)$. This picture holds also during a contact with the third beam (Fig. 4), which in practice immediately approaches a chaotic state. For $q_{10} = 1$ the first Hopf bifurcation is collapsed, in the spectrum of the top and middle beams a strong increase of noisy components is observed, and then the system moves into chaos (Fig. 5).

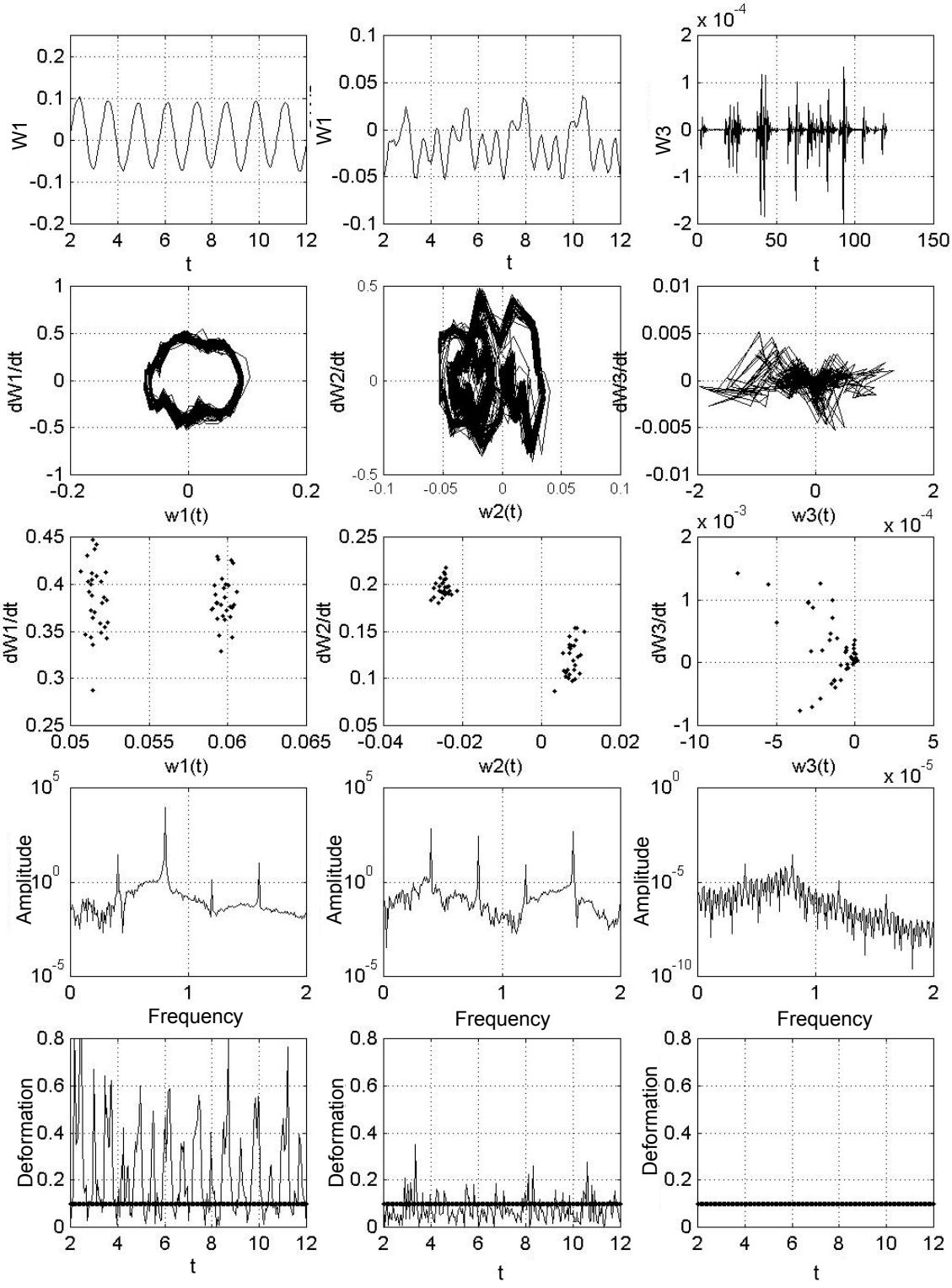

Figure 4. Vibrations $w_i(0.5;t)$, velocities $\dot{w}_i(0.5;t)$, Poincaré sections $(\dot{w}_i, w_i)$ and power spectra for $q_1 = 0.80$.

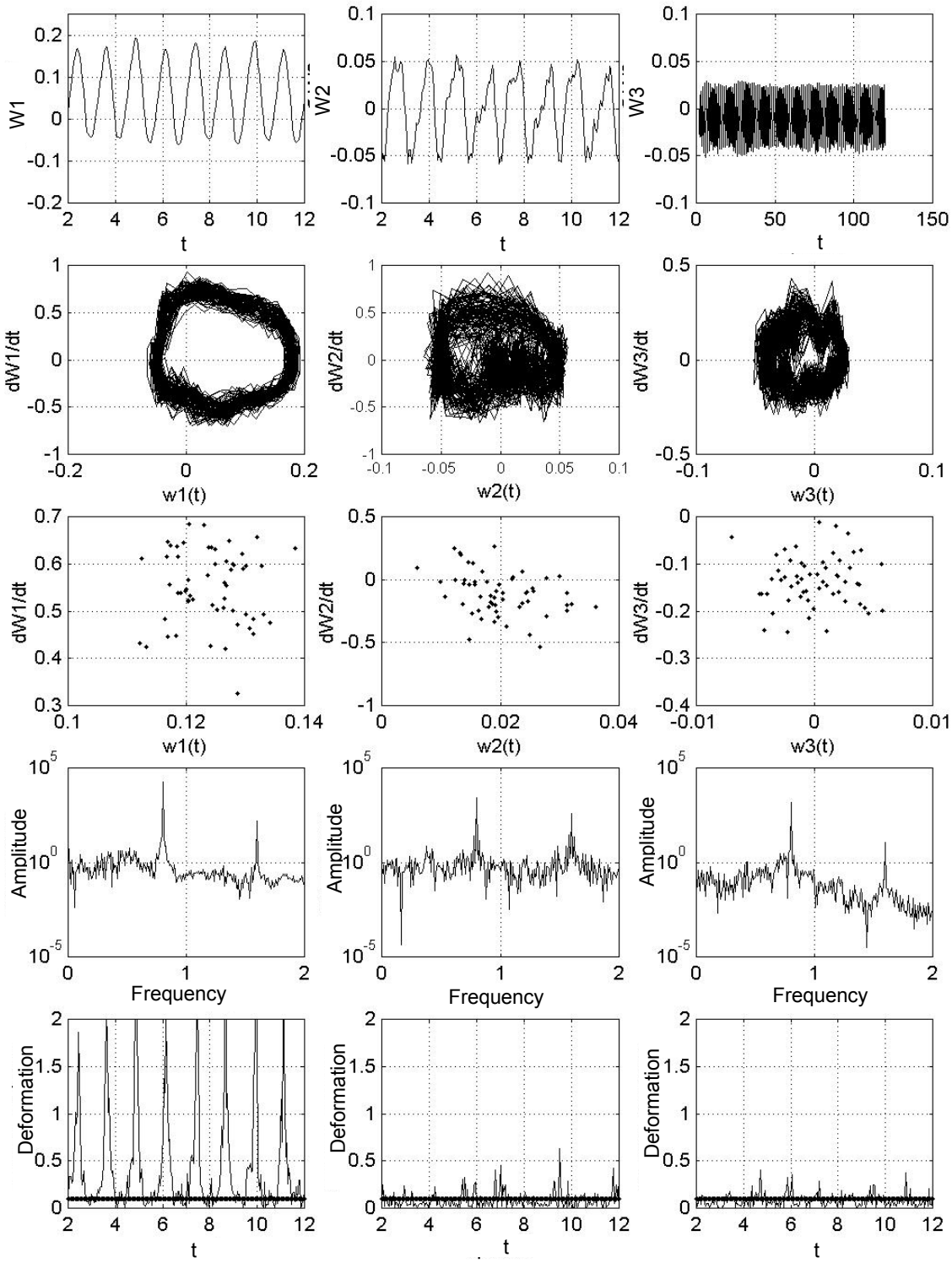

Figure 5. Vibrations $w_i(0.5;t)$, velocities $\dot{w}_i(0.5;t)$, Poincaré sections $(\dot{w}_i, w_i)$ and power spectra for $q_1 = 1.5$.

To conclude, the increase of the parameter q_{10} is accompanied by a motion at low scales. The higher frequencies appear and the beams motion is more complex. In the power spectrum a transition from the

discrete to the continuous spectrum is observed, and it is widened into a set of high frequencies. During a transition to chaos, and occurrence of large motions, the shape of the power spectrum recalls that of the processes where the energy cascades into the top of spectrum. In other words, clearly expressed maximum, with mild decrease of the spectrum density in direction of high frequencies, and a sudden decrease in the direction of low frequencies is observed. The increase of q_{10} is accompanied by a shift of the spectrum density maximum in direction of high frequencies.

It should be emphasized, that energy cascade into the high part of the spectrum is typical for continuous systems exhibiting complex dynamics, including hydrodynamic objects.

Note that a route to chaos is different than in the case previously analyzed. The bifurcation series are not observed, and after the first Hopf bifurcation the system immediately transits to chaos. Therefore, the presence of non-linearly elastic material qualitatively changes the vibrational process.

6 Concluding Remarks

The general and high accuracy method to trace bifurcation and chaos of physically dissipative non-linear sandwich of three beams is proposed. First, the governing equations are derived and the computational finite difference algorithm is described. Three different materials of the beams are considered (ideally elastic-plastic, elastic-plastic with linear strengthens, and the pure aluminum). The amplitude characteristics, phase portraits, Poincaré sections and the power spectrum are used to trace bifurcations and chaos of the analysed system. Two main computational examples are reported. In the first one, the dynamics of linearly elastic beams is analysed. The periodic, quasi-periodic and chaotic dynamics of the beams is described in the text and it will be not repeated here. In addition, the contact zones between beams are traced. One frequency bifurcation, a first Hopf bifurcation, the triple bifurcation birth and collapse, a second Hopf bifurcation and its collapse, and the bifurcation scenario leading to chaos are illustrated and discussed, among others.

The second example includes three beams which are non-linearly elastic (detailed description is given in the latter section). In the beams power spectrum, a transition from the discrete to continuous spectrum is observed with a clearly exhibited energy cascade into the high spectrum component. The bifurcation series scenario leading to chaos is not observed in this case. After the first Hopf bifurcation the system suddenly jumps straight into ‘chaos’.

References

[1] D. J. Mead, S. Markus, The forced vibration of three-layer, damped sandwich beam with arbitrary boundary conditions. *Journal of Sound and Vibration*, **10**: 163-175, 1969.

[2] D. J. Mead, S. Markus, Loss factors and resonant frequencies of encastré damped sandwich beams. *Journal of Sound and Vibration*, **12**: 99-112, 1970.

[3] D. J. Mead, A comparison of some equations for the flexural vibration of damped sandwich beams. *Journal of Sound and Vibration*, **83**: 363-377, 1982.

[4] B. E. Douglas, J. C. S. Yang, Transverse compressional damping in the vibratory response of elastic-viscoelastic-elastic beams. *AIAA Journal*, **16**: 925-930, 1978.

[5] B. E. Douglas, Compressional damping three-layer beams incorporating nearly incompressible viscoelastic cores. *Journal of Sound and Vibration*, **104**: 343-347, 1986.

[6] C. L. Sisemore, A. A. Smaili, C. M. Darvennes, Experimental measurement of compressional damping in an elastic-viscoelastic-elastic sandwich beams. *Proceedings of the American Society of Mechanical Engineers Noise Control and Acoustics Division*, 1999, pp. 223-227.

[7] C. L. Sisemore, A. A. Smaili, J. R. Houghton, Passive damping of flexible mechanism systems: experimental and finite element investigations. *Proceedings of the Tenth World Congress of the Theory of Machines and Mechanisms*, 1999, 2140-2155.

[8] C. L. Sisemore, C. M. Darvennes, Transverse vibration of elastic-viscoelastic-elastic sandwich beams: compression-experimental and analytical study. *Journal of Sound and Vibration*, **252**: 155-167, 2002.

[9] Y. Chen, On the vibration of beams or rods carrying a concentrated mass. *American Society of Mechanical Engineers Journal of Applied Mechanics*, **30**(2): 310-312, 1963.

[10] R. P. Goel, Vibrations of a beam carrying a concentrated mass. *American Society of Mechanical Engineers Journal of Applied Mechanics*, **40**(3): 821-822, 1973.

[11] B. R. Bhat, H. Wagner, Natural frequencies of a uniform cantilever with a tip mass slender in the axial direction. *Journal of Sound and Vibration*, **45**: 304-307, 1976.

[12] B. R. Bhat, M. A. Kulkarni, Natural frequencies of a cantilever with a slender tip mass. *AIAA Journal*, **14**: 536-537, 1976.

[13] K.-T. Chan, X.-Q. Wang, T.-P. Leung, Free vibrations of a Timoshenko beam partially loaded with distributed mass. *Journal of Sound and Vibration*, **206**(3): 353-369, 1997.

[14] Ch K.-T. Chan, X.-Q. Wang, T.-P. Leung, Free vibrations of beams with two sections of distributed mass. *ASME Journal of Vibration and Acoustics*, **120**: 944-948, 1998.

[15] O. Kopmaz, S. Telli, On the eigenfrequencies of a two-part beam-mass system. *Journal of Sound and Vibration*, **252**: 370-384, 2002.

[16] Q. S. Li, Free vibration analysis of non-uniform beams with an arbitrary number of cracks and concentrated masses. *Journal of Sound and Vibration*, **252**(3): 509-525, 2002.

[17] S. W. Shaw, C. Pierre, Normal modes for non-linear continuous systems. *Journal of Sound and Vibration*, **169**(3): 319-347, 1994.

[18] W. C. Xie, H. P. Lee, S. P. Lim, Normal modes of a non-linear clamped beam. *Journal of Sound and Vibration*, **250**(2): 339-349, 2002.

[19] T. A. Doughty, P. Davies, A. K. Bajaj, A comparison of three techniques using steady state data to identify non-linear modal behavior of an externally excited cantilever beam. *Journal of Sound and Vibration*, **249**(4): 785-813, 2002.

[20] M. A. Heckl, Coupled waves on a periodically supported Timoshenko beam. *Journal of Sound and Vibration*, **252**(5): 849-882, 2002.

[21] H. Matsunaga, Vibration and buckling of multilayered composite beams according to higher order deformation theories. *Journal of Sound and Vibration*, **246**(1): 47-62, 2001.

[22] O. J. Aldraiham, A. Baz, Dynamic stability of stepped beams under moving loads. *Journal of Sound and Vibration*, **250**(5): 835-848, 2002.

[23] D. J. Mead, Free vibrations of self-strained assemblies of beams. *Journal of Sound and Vibration*, **249**(1): 101-127, 2002.

[24] V. V. Kovtunov, Chaotic vibrations of parametrically stabilized beam. *Strength of Materials and Theory of Constructions*, **59**: 83-87, 1991, in Russian.

[25] K. Nagai, T. Yamaguchi, Chaotic vibrations of past-buckled beam with a variable cross section under periodic exitution. *Trans. Jap. Soc. Mech. Eng. C*, **61**(586): 2202–2209, 1995.

[26] K. Nagai, T. Yamaguchi, Chaotic vibrations of past-buckled beam carring a concentrated mass//Experiment. 1-st report. *Trans. Jap. Soc. Mech. Eng. C*, **61**(579): 3733-3740, 1994.

[27] T. Yamaguchi, K. Nagai, Chaotic vibrations of past-buckled beam carring a concentrated mass. II-end report. Theoretical analysis. *Trans. Jap. Soc. Mech. Eng. C*, **61**(579): 3741-3748, 1994.

[28] K. Yagasaki, Bifurcations and chaos in quasi-periodically forced beam, Theory, simulation and experiment. *Journal of Sound and Vibration*, **183**(1): 1-31, 1995.

[29] K. Nagai, K. Kasuga, M. Kamada, T. Yamaguchi, K. Tanifuji, Experiment on chaotic oscillations of a post-buckled reinforced beam constrained by an axial spring. *Jap. Soc. Mech. Eng. Int. J. C.*, **41**(3): 563-569, 1998.

[30] B. Ya. Kantor, *Contact Problems of Nonlinear Theory of Rotational Shells*. Naukowa Dumka, Kiev, 1990.

[31] V. A. Krysko, *Nonlinear Static and Dynamics of Non-Homogeneous Shells*. Saratov University Press, Saratov, in Russian, 1976.